JOURNAL OF Materials CHEMISTRY

In situ X-ray absorption spectroscopic studies at the cobalt K-edge on an Al_2O_3-supported rhenium-promoted cobalt Fischer–Tropsch catalyst. Comparing reductions in high and low concentration hydrogen

Arild Moen,[a] David G. Nicholson,[a] Magnus Rønning[b] and Hermann Emerich[c]

[a] *Department of Chemistry, Norwegian University of Science and Technology, N-7055 Trondheim, Norway*
[b] *Department of Industrial Chemistry, Norwegian University of Science and Technology, N-7055 Trondheim, Norway*
[c] *Swiss-Norwegian Beamline, European Synchrotron Radiation Facility BP 220, F-38043 Grenoble, France*

Received 5th June 1998, Accepted 10th August 1998

In situ XAFS spectroscopic studies have been carried out at 450 °C on the hydrogen reduction of a rhenium-promoted Co_3O_4/Al_2O_3 catalyst. Reductions carried out using 100% hydrogen and 5% hydrogen in helium gave different results. Whereas the reduction using dilute hydrogen yielded bulk-like metallic cobalt particles (hcp or fcc), the reaction with pure hydrogen led to a more dispersed system with smaller cobalt metal particles (<40 Å) the crystal form of which could not be established so that the recently reported metastable nonclose-packed body-centred cubic form cannot be excluded. Reoxidation of a similar catalyst in water-containing gas mixtures has been reported in the literature; it is suggested that the different outcome in the case of the 100% hydrogen protocol may be due to a similar mechanism. This would involve the *in situ* water produced by the reduction with reoxidation–reduction of cobalt metal particles in the water vapour–hydrogen mixture. However, this mechanism cannot be established by the present study. Additionally, in both reduction protocols a small fraction (3–4 wt.%) of the cobalt content is randomly dispersed over the tetrahedral vacancies of the alumina support with Co–O bond lengths of 1.96 ± 0.01 Å. This dispersion occurs during reduction and not calcination.The cobalt in these sites cannot be reduced at 450 °C, a temperature that is too low to permit formation of the spinel $CoAl_2O_4$.

X-Ray absorption spectroscopy (XAS) is a useful method for characterising local structural features of selected elements in heterogeneous catalysts. Although the technique is actually a bulk technique it is also valuable for studying chemical reactions that take place at the surfaces of heterogeneous catalysts because the overall contribution to the XAS signal arises from the significant proportion of active sites that are highly dispersed over a large number of surfaces. Indeed, XAS is particularly suited for characterising such systems because their inherent lack of long range order precludes study by X-ray diffraction. In addition, XAS is capable of giving information on interactions between the support and the metal catalyst, an aspect which is relevant to this work since such interactions are known to influence activity and selectivity.[1–3]

This paper is concerned with an alumina-supported cobalt catalyst used in the Fischer–Tropsch process. In this process linear high-molecular weight aliphatic hydrocarbons are synthesised by catalytically hydrogenating carbon monoxide.[4–30] A comprehensive review of the literature dealing with this system and its variants is given by Holmen *et al.*[31]

XAS has been used previously to study several modifications of Co/Al_2O_3 catalysts. Probably the earliest study was that reported by Greegor *et al.*[32] Fay *et al.*[24] used the method to characterise a boron-modified system, and Huffman *et al.*[33] used XAS in an *in situ* study of potassium-promoted cobalt catalysts supported on alumina and silica during reduction in hydrogen at 200 °C with subsequent reaction in a synthesis gas mixture. The latter support was also used by Takeuchi *et al.*[34] Recently, Moen *et al.*[35] in a preliminary report described an *in situ* XAS study at the Co K-edge on the reduction of the rhenium-promoted Co/Al_2O_3 catalyst (cobalt content 26 wt.%) at 450 °C using 100% hydrogen.

From these studies it appears that catalyst preparation in part involves the diffusion of cobalt ions into the structure of γ-Al_2O_3 where they occupy vacant octahedral and/or tetrahedral positions. This apparently leads to two main types of cobalt-containing phase: (a) cobalt bonded to the alumina support in the form of a surface phase that is resistant to reduction and (b) the easily reduced spinel Co_3O_4 which dominates above a certain cobalt concentration (3–4%). A major factor determining catalytic activity is the influence of promotors; *e.g.* there is a two-fold increase in the rates of hydrogenation of carbon monoxide in the presence of platinum and rhenium promoters.[28,29]

We report here the results of *in situ* XAS experiments on the reduction with dilute hydrogen (5% in helium) at 450 °C of the rhenium-promoted Co/Al_2O_3 (cobalt content 26 wt.%). This is an extension of previous work[35] in which the catalyst was reduced by 100% hydrogen at the same temperature. We also report here the results of experiments carried out at lower temperatures (200 °C) on the same catalyst and the results of the reduction at 450 °C of a similar system but one with a much lower cobalt content (4.6%).

Experimental

Synthesis

Essentially following the procedure described in the literature[29] (but in our case with a triple cobalt loading) the alumina-supported cobalt catalyst with 26% cobalt loading (analysis by atomic absorption spectroscopy) was prepared by the incipient wetness impregnation of γ-alumina (sieved to 40–50 mesh) with aqueous solutions of $Co(NO_3)_2 \cdot 6H_2O$ and $HReO_4$ (calculated to give 1.0 wt.% rhenium). The resulting material was dried overnight at 120 °C and then calcined at

500 °C for 8 h. A sample of the same system but with a much lower cobalt loading (4.6%) was prepared and treated similarly.[29]

Hydrogen reduction of the catalysts was carried out *in situ* (see below).

X-Ray absorption data

XAS data were collected using the facilities of the bending magnet Swiss-Norwegian Beamline (SNBL) at the European Synchrotron Radiation Facility (ESRF), Grenoble, France. Spectra were obtained on station EH1 (SNBL-ESRF) at the cobalt K-edge ($\lambda = 1.6086$ Å; energy = 7 709 eV).

A channel-cut silicon(111) monochromator with an unfocussed beam was used to scan the X-ray spectra. The beam currents ranged from 80–130 mA at 6.0 GeV. Higher-order harmonics (*ca.* two orders of magnitude) were rejected by means of a gold-coated mirror angled at 7.3 mrad from a beam of size 0.6×4.7 mm which was defined by the slits in the station. The maximum resolution ($\Delta E/E$) of the Si(111) bandpass is 1.4×10^{-4}.

Gas ion chamber detectors with their gases at ambient temperature and pressure were used for measuring the intensities of the incident (I_0) and transmitted (I_t) X-rays. The detector gases were as follows: I_0, detector length 17 cm, 100% N_2; I_t, length 31 cm, 35% Ar, 65% N_2.

Data collected at the Co K-edge. The spectral energy calibration was checked by measuring the spectrum of a Co-foil (thickness 5 μm; the energy of the first inflection point being defined as the edge 7 709 eV; accurate calibrations are particularly important for the pre-edge and XANES regions where the need for comparisons between the different spectra make it necessary to define the absolute energies of the spectral features; for the EXAFS the energy is relative to the individual edges which are therefore defined as zero). The energy scale calibration of each spectrum was carried out using an in-house program.

The XAS of the catalysts, before and after reduction, and of the model compounds $CoAl_2O_4$, CoO, the cobalt Tutton salt, $[NH_4]_2[Co(H_2O)_6][SO_4]_2$, and Co_3O_4 were also measured. The amounts of material in the samples were calculated from element mass fractions and the absorption coefficients of the constituent elements[36] above the absorption edge to give an absorber optical thickness of 1.5 absorption lengths. The well-powdered samples of the model and reference compounds were mixed with boron nitride so as to give a sample thickness of *ca.* 1.0 mm and placed in aluminium sample holders and held in place by Kapton tape. Co_3O_4/Al_2O_3 destined for the *in situ* reduction was ground and sieved (7–125 μm) and mixed with the requisite amount of boron nitride or graphite to achieve the desired absorber thickness. (The experiment using graphite was to establish whether that material affects the product; the spectra of the samples diluted with boron nitride and graphite were similar.)

The catalyst was then loaded into a Lytle *in situ* reactor-cell[37] and reduced in a mixture of H_2 (5%) in He (purity; 99.995%: flow rate 60 ml min^{-1}) by heating from room temperature to 450 °C and maintaining at that temperature for 6 h.

The same procedure was repeated for other samples but with the difference that the hydrogen flow was started at 450 °C. Similar measurements were also carried out at 200 °C and for 13 h. The samples are designated as follows. Sample A: the catalyst containing 26% cobalt (shown below to be mainly Co_3O_4/Al_2O_3). Sample B: produced by reducing sample A in 100% hydrogen at 450 °C.[35] Sample C: prepared by reducing sample A in 5% hydrogen at 450 °C. Sample D was prepared by reducing the catalyst containing 4.6% cobalt in 5% hydrogen at 450 °C.

EXAFS data analysis. The data were corrected for dark currents, converted to k-space, summed and background subtracted to yield the EXAFS function $\chi^{obs}{}_i(k)$ using the EXCALIB and EXBACK programs.[38] Model fitting was carried out with EXCURV90 using curved-wave theory and *ab initio* phase shifts.[38,39] The edge positions were determined from the first inflection points (after any pre-edge features) of the derivative spectra.

The k^3 weighting scheme compensates for the diminishing photoelectron wave at higher k. The curve-fitting was performed on data that had been Fourier filtered over a wide range (1.0–25.0 Å). This filter removes low-frequency contributions to the EXAFS below 1 Å, but does not smooth the spectrum (*i.e.* the noise is not removed). The ranges for the Fourier transformations were 3–14 Å^{-1}.

The model compounds, cobalt Tutton salt,[40] cobalt aluminate[41] and cobalt(II) oxide[42] were used to check the validity of the *ab initio* phase shifts and establish the general parameter AFAC (proportion of absorption causing EXAFS) and VPI (allows for inelastic scattering of the photoelectron).[38] The cobalt spinel (Co_3O_4), which contains both cobalt(II) and cobalt(III),[43] was used as a reference.

Results and discussion

We have previously shown[35] that the XAS of the unreduced material (sample A) is indistinguishable from that of the reference compound Co_3O_4. Clearly, the method of preparation, together with the comparatively high cobalt loading, yields a material in which Co_3O_4 is the dominant phase and that this phase is distributed throughout sample A in the form of relatively large (>100 Å) crystallites. This conclusion is consistent with the sizes (140–190 Å) derived from the line broadening observed in the X-ray diffractogram.[29]

The reduction at 450 °C with 5% hydrogen was monitored by a series of quick short scans taken just before and after the edge. The intensity of the white line (characteristic of Co_3O_4) rapidly decreased with time and on the basis of this indicator the reduction was essentially completed within approximately 15 min, although the process was continued for a further 6 h.

Fig. 1 shows the XAS of sample A (26 wt.% loading of cobalt) reduced by 100% and 5% hydrogen (to give samples B and C, respectively) and sample D (4.6 wt.% loading) reduced in 5% hydrogen; the spectrum of bulk cobalt metal is also shown. The X-ray absorption near edge structure (XANES) regions for the model/reference compounds and samples A, B, C, D are depicted in Fig. 2. The model/reference compounds, chosen for their tetrahedral and octahedral cobalt environments, are represented by the following compounds: $CoAl_2O_4$ (tetrahedral $Co^{II}(O)_4$); $[NH_4]_2[Co(H_2O)_6][SO_4]_2$ (distorted octahedral $Co^{II}(O)_6$); CoO (octahedral $Co^{II}(O)_6$); and Co_3O_4 (tetrahedral $Co^{II}(O)_4$ plus octahedral $Co^{II}(O)_6$). Fig. 3 contains the first derivatives of the edge region because they are useful for highlighting characteristic features about the edges (particularly the pre-edge features) and establishing their energies.[35,44]

A comparison of the XAS of cobalt metal (as a foil with the face centred cubic or hexagonal close-packed structure, their spectra are similar[35]) and sample B in Fig. 1 reveals that there are significant differences between them. Yet, the spectrum of sample C closely resembles that of the cobalt metal. The edge regions of bulk cobalt metal and sample B are also different, as emphasised by the first derivatives (Fig. 3). Evidently, sample B, unlike sample C, is not composed of bulk metal particles. Hence, reduction by 100% and 5% hydrogen yields products (B and C) with different physical characteristics.

The most prominent features in the XAS of sample B are the pre-edge peak at 7709 eV and the absence (or considerable reduction) of the white line so characteristic of Co_3O_4,

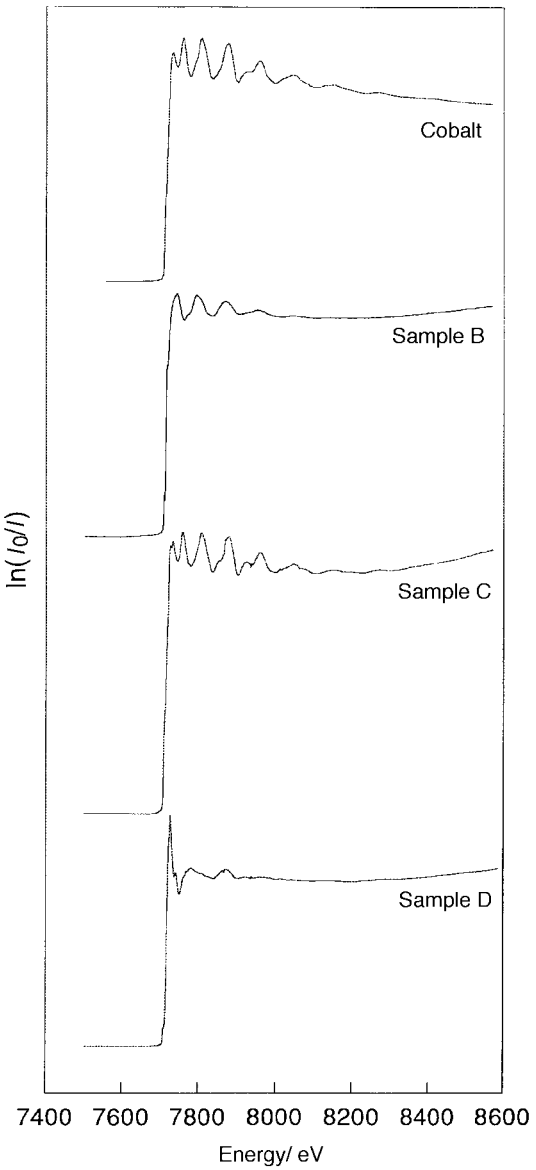

Fig. 1 Normalised XAS of samples B, C, D and the reference cobalt metal.

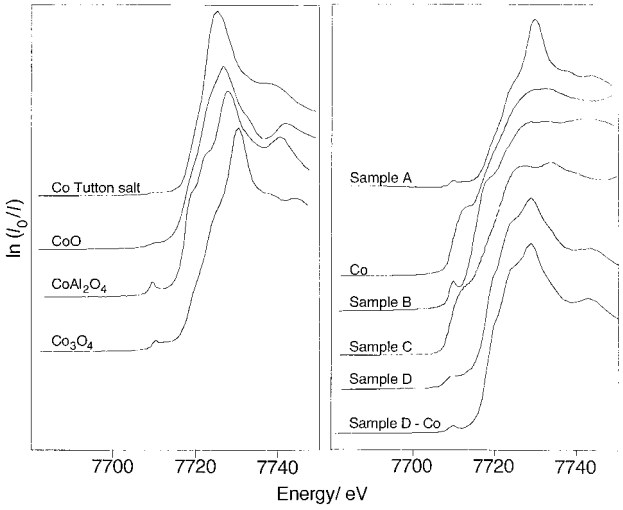

Fig. 2 Normalised Co K-edge XANES of the samples and reference materials.

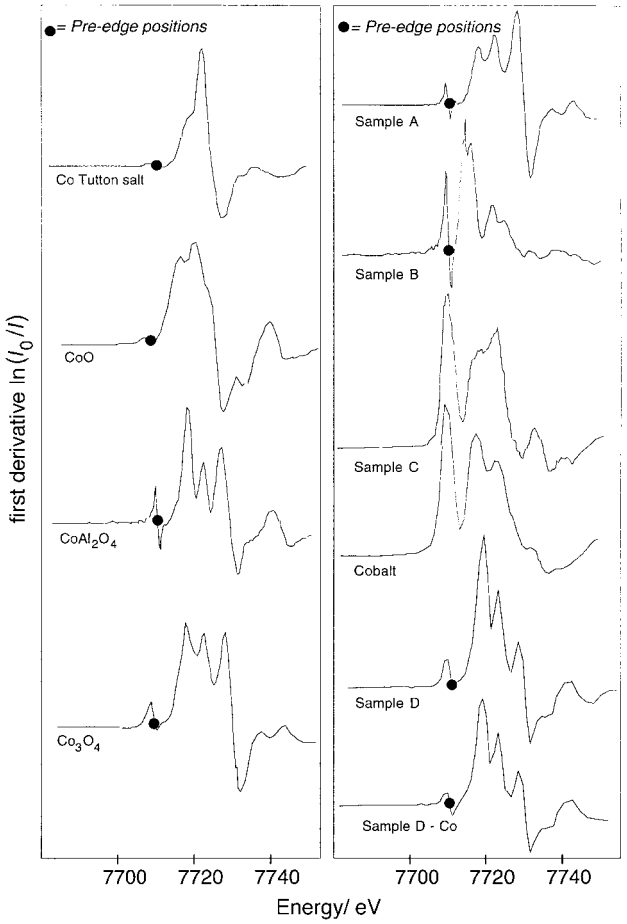

Fig. 3 The first derivatives of the XANES spectra of samples A, B, C, D and the reference/model compounds. The positions of the pre-edge peaks are marked (●).

$CoAl_2O_4$, CoO, cobalt Tutton salt and its precursor, sample A. The white line is also absent in the XAS of bulk cobalt metal which suggests that sample B contains a high degree of reduced material consistent with the estimate (80%) for reducibility of rhenium-promoted Co_3O_4/Al_2O_3 under the same conditions.[29]

Pre-edge peaks

The XAS at the K-edge of certain valence states of some transition compounds often contain an electronically interesting pre-edge feature a few eV below the edge. This feature is useful because it yields structural and electronic information, especially when combined with the extended X-ray absorption fine structure (EXAFS) region of the same spectrum.[44,45]

The peak results from the absorption process 1s→3d and for solid macromolecular materials (such as CoO, $CoAl_2O_4$ and Co_3O_4) the final state(s) are unoccupied bands. The transition probability (intensity) is related to the symmetry ($A_1 \rightarrow T_2$ for T_d symmetry) and to the occupancy of the 3d shell. For a given occupancy, the transition is most intense when the first coordination shell lacks inversion symmetry. In the case of the cubic point groups this applies to tetrahedral (T_d) environments but not to octahedral (O_h) symmetry; although for the latter point group a considerably weaker pre-edge feature does actually occur (despite being forbidden by the centre of symmetry). This is because the crystallographic point group represents a static model derived by time-averaging the asymmetric vibrations within the molecule whereas the XAS reacts to the individually and constantly changing structures of the local environment as vibrations momentarily eliminate the centre of symmetry. An example is the spectrum

(Fig. 2 and 3) of CoO, with its very weak pre-edge feature (better revealed in the derivative of the spectrum), in which the octahedrally coordinated cobalt is in an O_h environment.[44]

For symmetries lower than O_h, as in the distorted octahedrally coordinated cobalt environment ($Co(H_2O)_6^{2+}$) in the Tutton salt, $[NH_4]_2[Co(H_2O)_6][SO_4]_2$,[40] the intensity is somewhat enhanced, although still comparatively weak.

By contrast, the pre-edge peaks associated with tetrahedral cobalt environments are more intense in accordance with the noncentrosymmeric T_d point group. This is exemplified in the spectrum of $CoAl_2O_4$ (Fig. 2 and 3). These figures also show the pre-edge region for the spinel Co_3O_4 which has one third cobalt(II) in tetrahedral sites and two thirds Co(III) in octahedral sites. The pre-edge feature is composed of the tetrahedral peak and the very weak (forbidden) octahedral peak, the overall peak intensity being reduced because the proportion of the cobalt content in tetrahedral sites is now only one third the total cobalt content and not unity as in $CoAl_2O_4$ (but see below).

XAS of sample B

Fig. 4 shows the XANES regions of samples A and B and bulk cobalt metal. The edge position of sample B is at a higher energy (7714 eV) than that in bulk cobalt metal. The pre-edge peak at 7710 eV in sample B serves both as a convenient control of the edge energy and as an important diagnostic feature for tetrahedral $Co^{II}(O)_4$ environments. Another significant feature in the sample B spectrum is the absence of the white line. As shown in the same figure, this is also characteristic of bulk metallic cobalt. Since the edge energy of bulk metallic cobalt is 7 709 eV, any significant contribution from that metal in a composite spectrum of two-or-more phases would obscure this pre-edge peak. This does not occur in sample B because the edge is actually moved to a higher energy. The significance of the edge shift, the pre-edge peak and a considerably reduced EXAFS amplitude have been discussed in terms of small metal particles (<40 Å) and the consequent deviation from bulk properties.[35] The effect of particle size on the EXAFS amplitude is significant for dimensions below *ca.* 30 Å.[26] Recent studies on the size determination by EXAFS confirm this.[46]

It is therefore apparent that a minor fraction of cobalt in sample B is sited in the tetrahedral environment that we know is present from the pre-edge peak. The distances extracted[35] from the EXAFS are 1.92 ± 0.01 Å (Debye–Waller type factor $(2\sigma^2) = 0.011$ Å^2) for the $Co(O)_4$ tetrahedral site (which is close to the distance extracted from the cobalt-containing support in sample D, see below) and 2.49 ± 0.01 Å (Debye–Waller type factor $(2\sigma^2) = 0.023$ Å^2) due to Co–Co backscattering. Whereas the former distance corresponds to the bond length of a tetrahedral $Co^{II}(O)_4$ environment the latter appears to be somewhat shorter than that yielded by the EXAFS of the bulk cobalt metal reference (2.48 ± 0.02 Å, Debye–Waller type factor $(2\sigma^2) = 0.013$ Å^2). Apai *et al.*[47] reported that metal–metal distances in very small metal particles are contracted relative to those in the bulk, an observation that has subsequently been reported by others.[48,49] Although a shortened Co–Co distance would accompany an edge shift a more detailed study that focuses on this particular aspect is required before the final conclusion can be drawn.

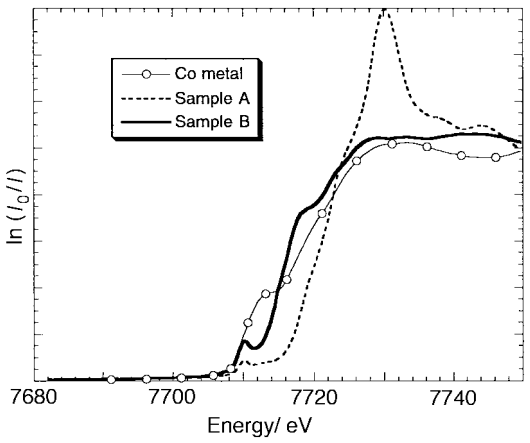

Fig. 4 Normalised Co K-edge XANES regions of samples A and B and the reference cobalt metal (bulk).

XAS of sample C

The XAS spectrum (Fig. 5 shows the magnitude of the Fourier transforms of the EXAFS region) of sample C shows that reduction at 450 °C in 5% hydrogen produces bulk-like cobalt metal (hcp or fcc) particles with only a minor fraction of cobalt being incorporated into the alumina support (the nonmetallic phase); the latter is discussed below.

XAS of sample D

It is evident from the full XAS spectrum (Fig. 1) and the EXAFS region (Fig. 6) that the major cobalt-containing component consists of cobalt incorporated into the alumina support. This cobalt fraction is not reduced by hydrogen at 450 °C. The pre-edge peak shows that the cobalt environment is tetrahedral $Co^{II}(O)_4$ the EXAFS yielding a Co–O distance of 1.96 ± 0.01 Å that is consistent with this.[43]

The effects of using concentrated *versus* dilute hydrogen

This study shows that the main reduction product of sample A at 450 °C using 100% hydrogen (sample B) differs from that

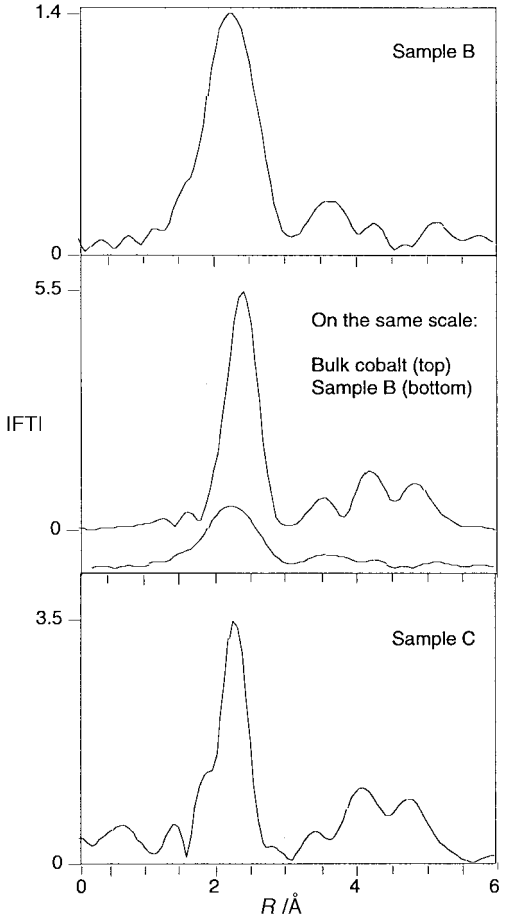

Fig. 5 Fourier transforms of samples B and C (top and bottom, respectively). The amplitudes of the peaks for sample B are much reduced compared with bulk cobalt metal (centre).

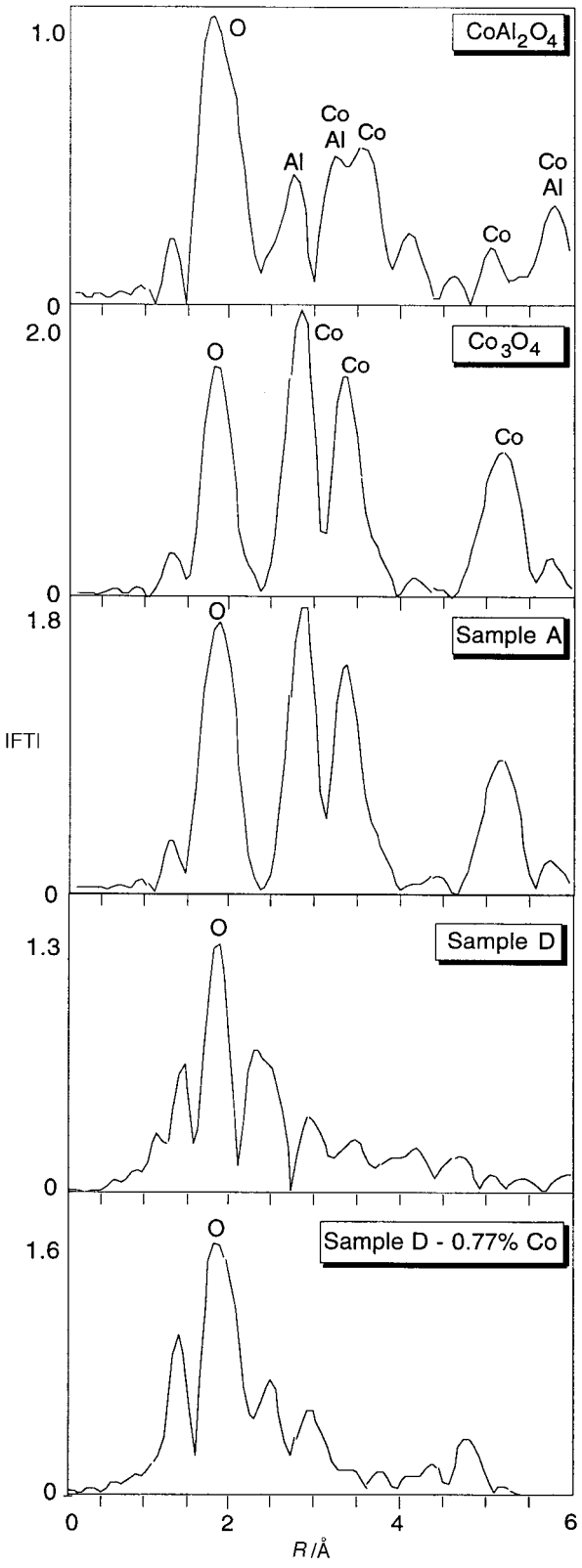

Fig. 6 Fourier transforms of sample A and sample D together with those of the spinel reference compounds.

obtained using 5% hydrogen in helium (sample C). An explanation for this difference is sought in a mechanism that we suggest may be connected with the reduction of this catalyst. Although the present results cannot establish this mechanism the concentration of hydrogen must be the key factor here. The background for the mechanism is provided by Hilmen *et al.*[50] who used temperature programmed reduction and gravimetry to show that cobalt is reoxidised in water-containing gas mixtures. They found that unpromoted and rhenium-promoted catalysts behave differently, with cobalt in the latter being more easily reoxidised and the resulting oxidised phase being more easily reduced. Other results in the literature also show that water has an effect; the introduction of water to Fischer–Tropsch reactions that are catalysed by variants of the Co/Al_2O_3 system affect the rate of reaction and distribution of the reaction products.[51,52]

Turning to the present experiments, since *in situ* water (*ca.* 2 mg) is produced during the reduction some degree of reoxidation of the freshly reduced cobalt metal would fit in with the results of Hilmen *et al.*[50] If the action of *in situ* water is responsible for the different outcomes of 100% and 5% hydrogen reduction at 450 °C then it seems likely that the partial pressures of water must be highest for the former and hence more effective in reoxidising metal particles which are again reduced by hydrogen.

Further experiments are necessary to ascertain whether this suggested mechanism is viable and also to establish whether a reoxidation–reduction process increases the metal dispersion by breaking up the initially large cobalt particles into smaller particles.

The nonmetallic phase

Information concerning the amount of cobalt incorporated into the alumina support is forthcoming from the XAS of samples C and D with 26% and 4.6% cobalt (as noted above). The data for the latter show that the amount of metallic cobalt produced is small. In order to estimate the fraction of cobalt that is incorporated into the alumina support the spectra of the high- and low-cobalt samples were first normalised and then a series of summed spectra were constructed by adding the low-cobalt spectrum (the major component in the support being cobalt incorporated into the support) to progressively increasing numbers of cobalt-metal spectra until the actual spectrum of the high-cobalt sample was closely reproduced. The best simulation was obtained with the fractions cobalt metal : low-cobalt catalyst being in the ratio 8 : 1. For the 26% loading this translates into *ca.* 3% cobalt being incorporated into the alumina support. (If the small fraction of metallic cobalt present in sample D (0.77%, see below) is taken into account then this figure would be slightly higher.)

In order to check this result, the following alternative procedure was used. On comparing the pre-edge regions of samples C and D (Fig. 2) it is evident that the pre-edge peak assigned to tetrahedral $Co(O)_4$ environments is obscured by the dominating contribution from metallic cobalt in the former (the position of the edge for cobalt metal being the same as that for the pre-edge peak.) Consistent with the low-cobalt metal content in sample D, the pre-edge peak in the spectrum of that material can be discerned because it is only partially merged into the metal edge. The spectrum of the nonmetallic phase was separated from the observed spectrum by subtracting the minor cobalt metal spectral contribution from the spectrum of sample D. The appropriately weighted cobalt-metal spectrum was obtained by multiplying the normalised cobalt-metal spectrum by a series of factors and subtracting each resulting spectrum from the actual spectrum of D until a spectrum (and its derivative) was obtained which exhibited a pre-edge peak that closely matched the same feature in $CoAl_2O_4$.

A good match was generated by subtracting the cobalt-metal spectrum weighted by the fraction 0.167 from the observed composite spectrum. This corresponds to a metal content of 0.77% cobalt for the 4.6% cobalt loading in sample D, the low-cobalt catalyst. (The same procedure has been described recently in ref. 44.) Hence, the nonmetallic phase contributes 3.8% to the total cobalt loading of the catalysts. This can be rationalised in terms of the structure of γ-alumina. The sup-

port, γ-Al_2O_3, has a defect spinel structure in which not all of the cation sites are occupied, *i.e.* $Al_{21\frac{1}{3}}\square 2_{2\frac{2}{3}}O_{32}$, where $\square$ designates vacant tetrahedral and octahedral sites.[53] If cobalt is distributed as Co(II) over the vacant tetrahedral sites in alumina (one third of the total vacant sites) then this would yield $Al^{III}{}_{21\frac{1}{3}}Co^{II}{}_{\frac{8}{9}}O_{32\frac{8}{9}}$, with the cobalt content being 4.5%, a value which is close to that found (3.8%) in the nonmetallic phase.

Thus, the data for the high and low-cobalt loadings are consistent with 3–4% cobalt being randomly dispersed over vacant tetrahedral sites of the alumina support. Fig. 7 shows the EXAFS and the magnitude of the Fourier transform together with the parameters obtained from the least-squares refinement. The Co–O bond distance (1.96 ± 0.01 Å) is typical for tetrahedral coordinated cobalt(II),[44] a similar value is also obtained for sample B (see above) and the pre-edge peak in that material's spectrum is consistent with some of the cobalt being incorporated in the support in a similar manner.

The XANES spectrum and its derivative of the cobalt-incorporated support (designated sample D − Co and obtained by removing the cobalt metal component from the spectrum of sample D) are shown in Fig. 2 and 3. There are marked similarities with the XANES of $CoAl_2O_4$. Like the latter the derivative spectrum is also consistent with a minor amount of cobalt entering some of the vacant octahedral sites of the bearer.[44]

It has been assumed that $CoAl_2O_4$ is the phase generated when cobalt occupies the vacant tetrahedral positions of the alumina lattice[28] but the present study clearly excludes the presence of $CoAl_2O_4$ in all of the reduced samples (B, C and D) (see Fig. 3 and 5) because the Co···Co distance in that compound is considerably longer (2.83 Å).[41] Instead, it is evident that only a small fraction of the total cobalt contents of samples B and C are randomly dispersed over vacant tetrahedral sites of the alumina support. This conclusion is supported by an X-ray diffraction study[57] which also shows that $CoAl_2O_4$ is not formed and additionally by the observation[28] that much higher calcination temperatures (>1200 °C) are needed to form $CoAl_2O_4$ from mixtures of Co_3O_4 and Al_2O_3.

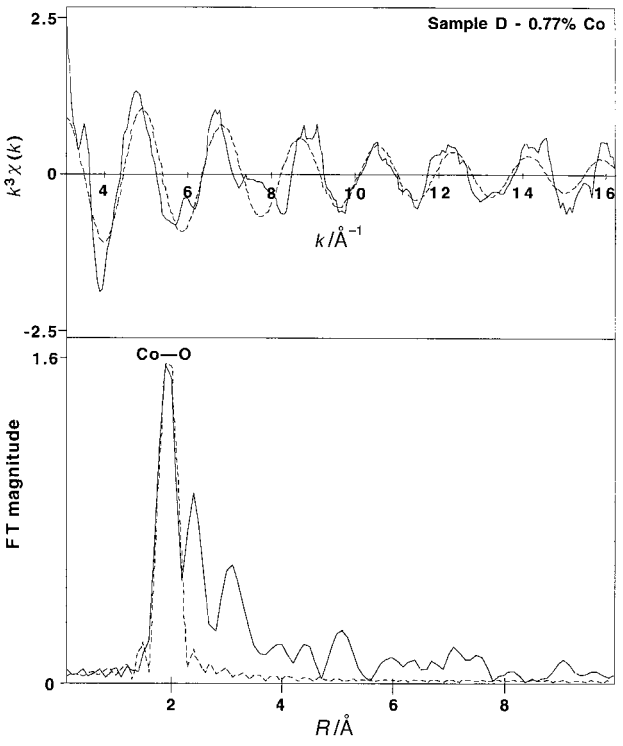

Fig. 7 (Top) k^3-Weighted experimental and least-squares fitted EXAFS of sample D adjusted for 0.77% cobalt metal (see main text). (Bottom) The magnitude of the Fourier transform (FT). The solid line shows the experimental data and the broken line represents the calculated EXAFS with its corresponding FT using a single Co–O shell. The final round of refinement yielded the following: distance $R_{Co-O} = 1.963(3)$ Å, coordination number $N = 3.2(2)$, and Debye–Waller-like factor $A = 2\sigma^2 = 0.0010(9)$ Å^2, and the refined correction to the threshold energy $E_0 = 21.98$ eV for an R-factor = 54.3%. The standard deviation in the last significant digit as calculated by EXCURV90 is given in parentheses. However, note that such estimates of precision (which reflect statistical errors in the fitting) overestimate the accuracy. The estimated errors for distances are 0.01 Å at $R < 2.5$ Å with 20% accuracy for N and A, although the accuracy for these is increased by refinements using k^1 *vs.* k^3 weighting.[44]

Reduction at 200 °C

Huffman *et al.*[33] reported that reduction of potassium-promoted Co_3O_4/Al_2O_3 at 200 °C yields cobalt-metal particles in which the coordination numbers are less than those for bulk cobalt metal. On this basis they estimated the average particle size to be as small as 10–20 Å although they doubted this estimate noting that the actual size must be larger. Unlike the present work, no other cobalt-containing phase was detected. The present study also differs in another respect since it shows that the rhenium-promoted Co_3O_4/Al_2O_3 catalyst is not reduced at 200 °C even when reacted with hydrogen for as long as 13 h.

The role of rhenium

In a temperature-programmed reduction (TPR) study of the mechanism of rhenium promotion of alumina-supported cobalt Fischer–Tropsch catalysts, Holmen *et al.*[31] reported that direct contact between rhenium and cobalt particles does not appear to be necessary for promotion. It is suggested that the mechanism by which rhenium promotes the reduction of Co_3O_4 is by hydrogen spillover. (The influence that rhenium exerts with regard to reduction and oxidation is mentioned above.) They also reported that cobalt diffuses into the support during the reduction and not during calcination which agrees with our findings. The increased dispersion that they found can account for the fact that the reduced rhenium-promoted catalyst relative to the unpromoted catalyst is consistent with the small particle sizes found in this XAS study.

Conclusion

XAS shows that high temperature reduction (450 °C) by 100% hydrogen of rhenium-promoted Co_3O_4/Al_2O_3 yields sample B which contains highly dispersed cobalt in the form of small (<40 Å) metal particles (Co–Co distance 2.49 ± 0.01 Å) together with a minor fraction of cobalt atoms that are randomly spread over the tetrahedral vacancies of the alumina support (Co(II)–O distance 1.92 ± 0.01 Å). The contribution to the XAS from this phase was isolated by reducing a catalyst in which essentially all of the cobalt entered the alumina support (sample D). These results are consistent with those of Holmen *et al.*[29–31] who found that the metal particles constitute 78% of the cobalt content. Also in agreement is the finding that cobalt diffuses into the support during reduction and not during calcination and that this phase is resistant to reduction at 450 °C and is not the spinel $CoAl_2O_4$.

A particularly interesting feature of the XANES of sample B is the 3–4 eV shift of the K-edge to higher energy relative to bulk cobalt metal. This, together with the reduced EXAFS amplitudes, is attributed to an enhanced dispersion of cobalt in the reduced material relative to the large bulk-like crystallites of Co_3O_4 the calcined product. This has been attributed to diminished shielding of the 1s electrons by the valence electrons which attends this heightened dispersion.[35] The higher dispersion and smaller particle sizes in sample B expresses the

positive effect that rhenium-promotion has on the reducibility of sample A.

No difference was observed when graphite was mixed with the catalyst instead of boron nitride. It is therefore clear that carbon does not play a role here in transforming the metal from the hexagonal or face-centred cubic structures to the metastable body-centred form (ref. 35 and refs. therein).

Support from the Nansen Foundation, the Norwegian Research Council (including a NATO Postdoctoral Fellowship to A. Moen) and VISTA-Statoil is much appreciated. The preliminary work (contribution No. 98-9) was carried out at the Swiss-Norwegian Beamline (SNBL) for which we thank the Norwegian University of Science and Technology and the Norwegian Research Council for grants towards its construction. We also thank the European Synchrotron Radiation Facility for beamtime (CH-440) on the SNBL. The assistance of the rest of the SNBL Project Team (K. Knudsen, P. Pattison and H.P. Weber) is also much appreciated and we thank Professor Anders Holmen for providing us with some of the samples.

References

1 F. Solymosi, *Catal. Rev.*, 1968, **1**, 233.
2 M. LoJacono and M. Schiavello, *Preparation of Catalysts*, ed. B. Delmon, P.A. Jacobs and G. Poncelot, Elsevier, Amsterdam, 1976, p. 473.
3 R. C. Reuel and C. H. Bartholomew, *J. Catal.*, 1984, **85**, 78.
4 J. H. Ashley and P. C. H. Mitchell, *J. Chem. Soc.*, *A*, 1968, 2821.
5 G. N. Asmolov and O. V. Krylov, *Kinet. Katal.*, 1971,**12**, 463.
6 H. Ueda and N. Todo, *J. Catal.*, 1972, **27**, 281.
7 M. LoJacono, J. L. Verbeek and G. C. A. Schuit, *J. Catal.*, 1973, **29**, 463.
8 J. Grimblot, J. P. Bonnelle and J. P. Beaufils, *J. Electron Spectrosc. Relat. Phenom.*, 1976, **8**, 473.
9 R. I. Declerck-Grimée, R. M. Caresson, R. M. Friedman and J. J. Fripiat, *J. Phys. Chem.*, 1978, **83**, 885.
10 P. Dufresne, J. Grimblot and J. P. Bonnelle, *Bull. Soc. Chim. Fr.*, 1980, **1**, 89.
11 K. S. Chung and F. E. Massoth, *J. Catal.*, 1980, **64**, 320.
12 K. S. Chung and F. E. Massoth, *J. Catal.*, 1980, **64**, 332.
13 R. B. Greegor, F. W. Lytle, R. L. Chin and D. M. Hercules, *J. Phys. Chem.*, 1981, **85**, 1232.
14 H. Topsøe, B. S. Clausen, R. Candia and C. Wivel, *J. Catal.*, 1981, **68**, 433.
15 N. Topsøe and H. Topsøe, *J. Catal.*, 1982, **75**, 354.
16 R. L. Chin and D. M. Hercules, *J. Phys. Chem.*, 1982, **86**, 360.
17 I. Alstrup, I. Chokendorft, R. Candia, B. S. Clausen and H. Topsøe, *J. Catal.*, 1982, **77**, 397.
18 C. Wivel, B. S. Clausen, R. Candia, S. Mørup and H. Topsøe, *J. Catal.*, 1984, **87**, 497.
19 P. Arnoldy and F. E. Massoth, *J. Catal.*, 1985, **93**, 38.
20 M. A. Stanick, M. Houalla and D. Hercules, *J. Catal.*, 1987, **103**, 151.
21 E. Garbowski, M. Guenin, M. Marion and M. Primet, *Appl. Catal.*, 1990, **64**, 209.
22 H. C. Tung, C. Yeh and C. T. Hong, *J. Catal.*, 1990, **122**, 211.
23 C. Bai, S. Soled, K. Dwight and A. Wold, *J. Solid State Chem.*, 1991, **91**, 148.
24 M. J. Fay, A. Procter, D. P. Hoffmann, M. Houalla and D. M. Hercules, *Appl. Spectrosc.*, **1992**, **46**, 345.
25 E. A. Blekkan, H. Holmen and S. Vada, *Acta Chem. Scand.*, 1993, **47**, 275.
26 M. Shirai, T. Inoue, H. Onishi, K. Asakura and Y. Iwasawa, *J. Catal.*, 1994, **145**, 159.
27 A. Kogelbauer, J. C. Weber and J. G. Goodwin, *Catal. Lett.*, 1996, **34**, 259.
28 P. G. Dimitrova and D. R. Mehandjiev, *J. Catal.*, 1994, **145**, 356.
29 S. Vada, A. Hoff, E. Ådnanes, D. Schanke and A. Holmen, *Top. Catal.*, 1995, **2**, 155.
30 D. Schanke, A. M. Hilmen, E. Bergene, K. Kinnari, E. Rytter, E. Ådnanes and A. Holmen, *Catal. Lett.*, 1995, **34,** 269.
31 A. M. Hilmen, D. Schanke and A. Holmen, *Catal. Lett.*, 1996, **34,** 143.
32 R. B. Greegor, F. W. Lytle, R. Chin and D. M. Hercules, *J. Phys. Chem.*, 1981, **85**, 1232.
33 G. H. Huffman, N. Shah, J. Zhao, F. E. Huggins, T. E. Hoost, S. Halvorsen and J. G. Goodwin, *J. Catal.*, 1995, **151**, 17.
34 K. Takeuchi, T. Hanaoka, T. Matsuzaki, M. Reinikainen and Y. Sugi, *Catal. Lett.*, 1991, **8**, 253.
35 A. Moen, D. G. Nicholson, B. S. Clausen, P. L. Hansen, A. Molenbroek and G. Steffensen, *Chem. Mater.*, 1997, **9**, 1241.
36 *International Tables for X-Ray Crystallography*, Kynoch Press, Birmingham, 1962, vol. 3, 175.
37 W. Lytle, R. B. Greegor, E. C. Marques, D. R. Sandstrom, G. H. Via and J. H. Sinfelt, *J. Catal.*, 1985, **95**, 546.
38 EXCALIB, EXBACK and EXCURV90 programs, N. Binsted, J. W. Campbell, S. J. Gurman and P. C. Stephenson, SERC Daresbury Laboratory, 1990.
39 S. J. Gurman, N. Binsted and I. Ross, *J. Phys. C: Solid State Phys.*, 1984, **17**, 143.
40 F. A. Cotton, L. M. Daniels, C. A. Murillo and J. F. Quesada, *Inorg. Chem.*, 1993, **32**, 4861.
41 K.Toriuma, M. Ozima, M. Akaogi and Y. Sato, *Acta Crystallogr., Sect. B*, 1978, **34**, 1093.
42 S. Sasaki, K. Fujino, and Y. Takeuchi, *Proc. Jpn. Acad., Ser. B*, 1979, **55**, 43.
43 N. N. Greenwood and A. Earnshaw, *Chemistry of the Elements,* Pergamon, Oxford, 1984, p. 1294.
44 Arild Moen, David G. Nicholson, M. Rønning, Geraldine M. Lamble, Jyh-Fu Lee and Hermann Emerich, *J. Chem. Soc., Faraday Trans.*, 1997, **93**, 4071.
45 A. Moen, D. G. Nicholson, M. Rønning, *J. Chem. Soc., Faraday Trans.*, 1995, **91**, 3189 and refs. therein.
46 M. Borowski, *J. Phys. IV*, 1997, **7**, **C2**, 259.
47 G. Apai, J. F. Hamilton, J. Stohr and A. Thompson, *Phys. Rev. Lett.*, 1979, **43**, 165.
48 H. Toepsoe, L. B. Hansen, P. Stoltze and J. K. Norskov, *Catal. Today*, 1994, **21**, 49.
49 S. Diaz-Moreno, D. C. Koningsberger and A. Munoz-Paez, *Nucl. Instrum. Methods Phys. Res., Sect. B*, 1997, **133**, 15.
50 A. M. Hilmen, D. Schanke and A. Holmen, *Stud. Surf. Sci. Catal.*, 1997, **107**, 237.
51 Exxon Research & Engineering Co., *US Pat.* 5 227 407, 1993.
52 Exxon Research & Engineering Co., *Eur. Pat.* 0 339 923 B1, 1989.
53 N. N. Greenwood and A. Earnshaw, *Chemistry of the Elements,* Pergamon, Oxford, 1984, p. 280.
54 S. E. Colley, R. G. Copperthwaite and G. J. Hutchings, *Catal. Today*, 1991, **9**, 203.

Paper 8/04261F